THE STUDY OF SUPERHEAVY ELEMENTS AT SHIP — RESULTS AND DEVELOPMENTS

Sigurd Hofmann

Gesellschaft für Schwerionenforschung (GSI)
Planckstrasse 1, D-64220 Darmstadt, Germany
e-mail: S.Hofmann@gsi.de

(Received September 11, 2002)

Dedicated to Adam Sobiczewski in honour of his 70th birthday

The nuclear shell model predicts that the next doubly magic shell-closure beyond ^{208}Pb is at a proton number between $Z = 114$ and 126 and at a neutron number $N = 184$. The outstanding aim of experimental investigations is the exploration of this region of spherical 'Superheavy Elements'. This article describes the experiments that were performed recently at the GSI SHIP. They resulted in an unambiguous identification of elements 110 to 112. They were negative so far in searching for elements 113, 116, and 118. The measured decay data are compared with theoretical predictions. Some aspects concerning the reaction mechanism and the use of radioactive beams are also presented.

PACS numbers: 23.60.+e, 25.70.–z, 25.85.Ca, 27.90.+b

1. Introduction

In recent years the exploration of superheavy elements (SHE) received increasing interest both from theoretical as well as experimental investigation and both from chemical as well as physical studies. The reasons for the activity awakened again are based mainly on technical developments in the field of computer power, accelerator techniques and detection sensitivity.

Using faster and bigger computers the *properties* of heavy nuclei are studied from multi-dimensional macroscopic-microscopic calculations [1–11], self consistent Skyrme–Hartree–Fock and relativistic mean field models [12–15]. The results reveal a rather complex structure of shell effects which determine the stability of nuclei in the superheavy region.

The most difficult problem, however, which is awaiting a theoretical solution, is the understanding of the *synthesis* of superheavy nuclei. The calculation of the involved dynamical processes on a microscopic level is presently the most challenging and work intensive task [16–29].

Successful methods for the laboratory synthesis of heavy elements have been fusion-evaporation reactions using heavy-element targets; recoil-separation techniques [30]; and the identification of the nuclei by generic ties to known daughter decays after implantation into position-sensitive detectors [31, 32]. Experiments at low cross-sections necessitate projectile beams of high intensity and stability. Although the intensity limits have not presently been reached, considerable improvements of accelerator techniques have been made in recent years.

In the following section a description is given of studies of elements 110 to 112 performed at GSI Darmstadt. In subsequent sections the measured data on the decay properties of heavy and superheavy nuclei are compared with theoretical descriptions. Nuclear reactions are discussed for the synthesis of SHEs using stable and radioactive beams. Finally, a summary and outlook are given.

2. Experimental results

In this section, recent results are presented dealing with the confirmation of elements 110 to 112. Detailed presentations of the properties of elements 107 to 109 and of earlier results on elements 110 to 112 were given in previous reviews [33, 34].

Element 110 was discovered in 1994 using the reaction ^{62}Ni + ^{208}Pb $\rightarrow$ $^{270}110^*$ [35]. A total of three decay chains were measured (see also remarks at the end of this section). The main experiment was preceded by a thorough study of the excitation functions for the synthesis of ^{257}Rf and ^{265}Hs in order to determine the optimum beam energy for the production of element 110. The data revealed that the maximum cross-section for the synthesis of element 108 was shifted to a lower excitation energy, different from the predictions of reaction theories.

The heavier isotope $^{271}110$ was synthesized with a beam of the more neutron-rich isotope ^{64}Ni [34]. The important result for the further production of elements beyond meitnerium was that the cross-section was enhanced from 2.6 pb to 15 pb by increasing the neutron number of the projectile by two, which gave hope that the cross-sections could decrease less steeply with more neutron-rich projectiles. However, this expectation was not proven in the case of element 112.

The even-even nucleus $^{270}110$ was synthesized using the reaction ^{64}Ni + ^{207}Pb [36]. A total of eight α-decay chains was measured during an irradiation time of seven days. Decay data were obtained for the ground-state and a high spin K isomer, for which calculations predict spin and parity 8^+, 9^- or 10^- [37]. The new nuclei ^{266}Hs and ^{262}Sg were identified as daughter products after α decay. Spontaneous fission of ^{262}Sg terminates the decay chain.

Element 111 was synthesized in 1994 using the reaction ^{64}Ni + ^{209}Bi $\rightarrow$ $^{273}111^*$. A total of three α chains of the isotope ^{272}111 were observed [38]. Another three decay chains were measured in a confirmation experiment in October 2000 [39].

Element 112 was investigated at SHIP using the reaction ^{70}Zn + ^{208}Pb $\rightarrow$ $^{278}112^*$ [40]. The irradiation was performed in January–February 1996. Over a period of 24 days, a total of 3.4×10^{18} projectiles were collected. One α-decay chain, shown in the left side of Fig. 1, was observed resulting in a cross-section of 0.5 pb. The chain was assigned to the one neutron-emission channel. The experiment was repeated in May 2000 aiming to confirm the synthesis of ^{277}112 [39]. During a comparable measuring time, but using slightly higher beam energy, one more decay chain was observed, also shown in Fig. 1. The measured decay pattern of the first four α decays is in agreement with the one observed in the first experiment.

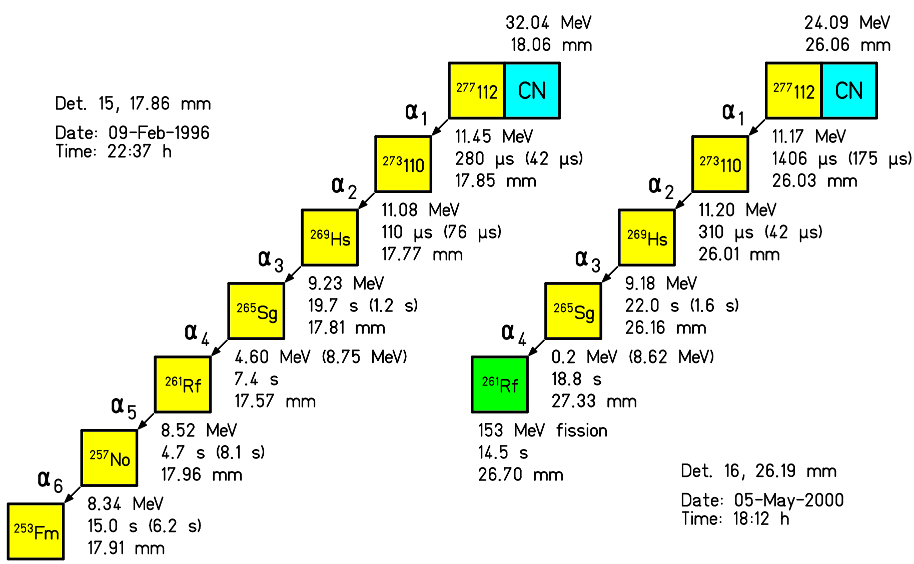

Fig. 1. Two decay chains measured in experiments at SHIP in the cold fusion reaction ^{70}Zn + ^{208}Pb $\rightarrow$ $^{278}112^*$. The chains were assigned to the isotope ^{277}112 produced by evaporation of one neutron from the compound nucleus. The lifetimes given in brackets were calculated using the measured α energies. In the case of escaped α particles the α energies were determined using the measured lifetimes.

A new result was the occurrence of fission which ended the second decay chain at ^{261}Rf. A spontaneous-fission branch of this nucleus was not yet known, however, it was expected from theoretical calculations. The new results on ^{261}Rf were proven in a recent chemistry experiment [41, 42], in which this isotope was measured as granddaughter in the decay chain of ^{269}Hs.

A reanalysis of all decay chains measured at SHIP since 1994, a total of 34 decay chains was analyzed, revealed that the previously published first decay chain of $^{277}112$ [40] (not shown in Fig. 1) and the second of the originally published four chains of $^{269}110$ [35] were spuriously created. Details of the results of the reanalysis are given in [39].

Results from an experiment at the 88-inch cyclotron in Berkeley aiming to synthesize element 118 were published in 1999 [43]. In order to confirm the data obtained in Berkeley, the same reaction, $^{86}\mathrm{Kr} + {}^{208}\mathrm{Pb} \to {}^{294}118^{*}$, was investigated at SHIP in the summer of 1999. The experiment is described in detail in Ref. [32]. During a measuring time of 24 days a beam dose of 2.9×10^{18} projectiles was collected, which was comparable to the Berkeley value of 2.3×10^{18}. No event chain was detected, and the cross-section limit resulting from the SHIP experiment for the synthesis of element 118 in cold fusion reactions was 1.0 pb. The Berkeley data were retracted in the summer of 2001 after negative results of a repetition experiment performed in the year 2001 in Berkeley itself and after a reanalysis of the data of the first experiment, which showed that the three reported chains were not in the 1999 data [44].

3. Nuclear structure and decay properties

The basic step which is necessary for the determination of the stability of SHEs is the calculation of the ground-state binding energy. As a signature for shell effects, we can extract from various models the shell-correction energy by subtracting a smooth macroscopic part (derived from the liquid-drop model) from the total binding energy. In macroscopic-microscopic models the shell-correction energy is of course the essential input value which is calculated directly from the shell model. The shell-correction energy is plotted in Fig. 2(a) using the data from Ref. [45]. Two equally deep minima are obtained, one at $Z = 108$ and $N = 162$ for deformed nuclei with deformation parameters $\beta_2 \approx 0.22$, $\beta_4 \approx -0.07$ and the other at $Z = 114$ and $N = 184$ for spherical SHEs. Different results are obtained from self-consistent Hartree–Fock–Bogoliubov (HFB) calculations and relativistic mean-field models [12–15]. They predict for the spherical nuclei shells at $Z = 114$, 120 or 126 (indicated as dashed lines in Fig. 2) and $N = 184$ or 172, with shell strengths being also a function of the amount of nucleons of the other type.

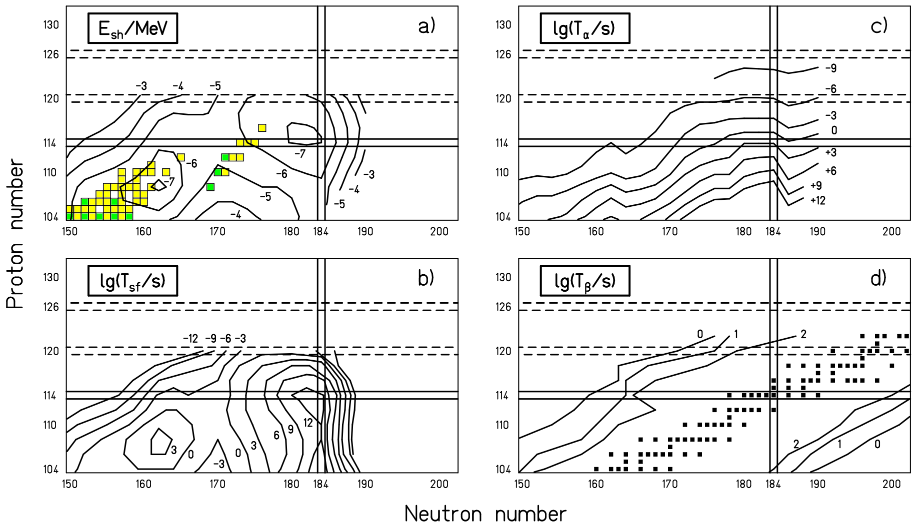

Fig. 2. Shell-correction energy (a) and partial spontaneous fission, α and β half-lives (b–d). The calculated values in (a)–(d) are taken from Refs [7, 45] and in (d) from Ref. [10]. The squares in (a) mark the nuclei presently known or under investigation.

For the calculation of partial spontaneous fission half-lives the knowledge of ground-state binding energies is not sufficient. It is necessary to determine the fission barrier over a wide range of deformation. The most accurate data were obtained for even-even nuclei using the macroscopic-microscopic model [7, 45]. Partial spontaneous fission half-lives are plotted in Fig. 2(b). The landscape of fission half-lives reflects the landscape of shell-correction energies, because in the region of SHEs the height of the fission barrier is mainly determined by the ground-state shell correction energy. The contribution from the macroscopic liquid-drop part approaches zero. Nevertheless we see a significant increase of fission half-life from 10^3 s for deformed nuclei to 10^{12} s for spherical SHEs. This difference is arising from the width of the fission barrier which becomes wider in the case of the spherical nuclei.

Partial α half-lives decrease almost monotonically from 10^{12} s down to 10^{-9} s near $Z = 126$ (Fig. 2(c)). The valley of β-stable nuclei (marked by black squares in Fig. 2(d)) passes through $Z = 114$, $N = 184$ [10]. At a distance from the bottom of the valley, the β half-lives decrease gradually down to values of one second.

The dominating partial half-life is shown in Fig. 3(a) for even-even nuclei. The two regions of deformed heavy nuclei near $N = 162$ and spherical SHEs merge and form a region of α emitters surrounded by fissioning nuclei. The longest half-lives are 1000 s for deformed heavy nuclei and 30 y for

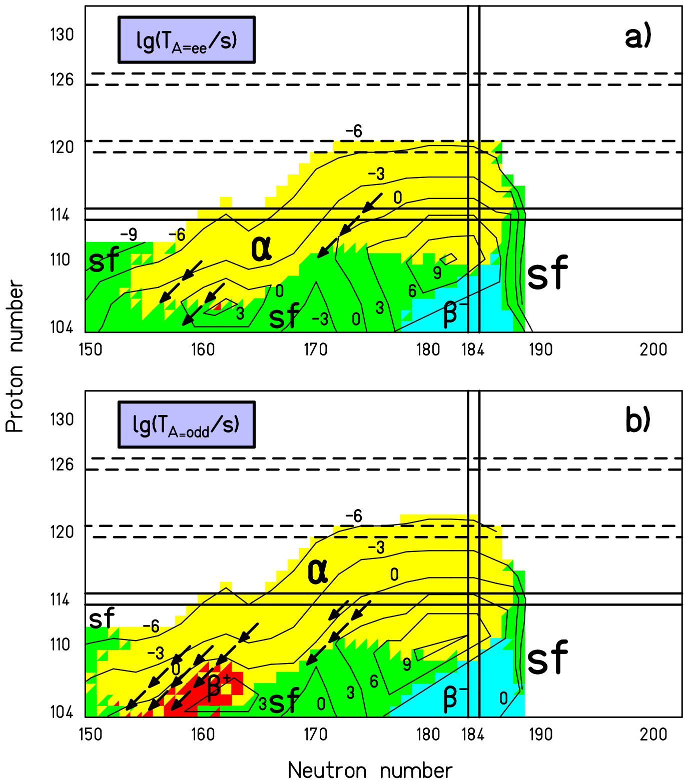

Fig. 3. Dominant half-lives for α, β^+/EC, β^- decay and spontaneous fission for even-even mass nuclei in (a) and for odd mass nuclei in (b). The arrows mark decay chains of nuclei presently known or under investigation.

spherical SHEs. It is interesting to note that the longest half-lives are not reached for the doubly magic nucleus $^{298}_{184}114$, but for $Z = 110$ and $N = 182$. This is a result of the increasing Q_α values with increasing element number. Therefore, the α decay becomes the dominant decay mode beyond element 110 with continuously decreasing half-life. The half-lives of nuclei at $N = 184$ and $Z < 110$ are reduced from β^- decay.

The four member decay chain of $^{292}116$, the heaviest even-even nucleus, observed in recent experiments in Dubna [46, 47] is also drawn in Fig. 3(a). The arrows follow approximately the 1-s contour line down to $^{280}110$, which is, in agreement with the experiment, predicted to be a spontaneously fissioning nucleus. The decay chains of two other recently synthesized even-even nuclei, $^{270}110$ [36] and ^{270}Hs [41, 42] are also drawn in the figure. In these cases the decay chains end by spontaneous fission at ^{262}Sg and ^{262}Rf, respectively.

In the case of odd nuclei (Fig. 3(b)), the α and fission half-lives calculated by Smolanczuk and Sobiczewski [7,45] were multiplied by a factor of 10 and 1000, respectively, thus making provisions for the odd particle hindrance factors. However, we have to keep in mind that the fission hindrance factors have a wide distribution from 10^1 to 10^5, which is mainly a result of the specific levels occupied by the odd nucleon. For odd-odd nuclei (not shown here), the fission hindrance factors from both the odd proton and the odd neutron are multiplied. The β half-lives given by Möller *et al.* [10] were divided by 10, because first-forbidden transitions were not taken into account in these calculations (see Möller *et al.* [10] and discussion therein).

For the odd and odd-odd nuclei, the island character of the α emitters disappeared and α decay could propagate down to rutherfordium and beyond. In the allegorical representation where the stability of SHEs is seen as an island in a sea of instability, the even-even nuclei portray the situation during a flood, the odd nuclei during an ebb, when the island is connected to the mainland.

The decay chains of the recently measured even-odd nuclei are also drawn in the figure: $^{277}112$, GSI [40], $^{287}114$ and $^{289}114$, JINR [48]. Here again, the measured data are predominantly well duplicated in the calculations.

The interesting question arises, if and how the uncertainty related with the location of the proton and neutron shell closures will change the half-lives of SHEs. Partial α and β half-lives are only insignificantly modified by shell effects, because the decay process occurs between neighboring nuclei. This is different for fission half-lives which are primarily determined by shell effects. However, the uncertainty related with the location of nuclei with the strongest shell-effects and thus longest partial fission half-life at $Z = 114$, 120 or 126 and $N = 172$ or 184, is inconsequential concerning the longest 'total' half-life of SHEs. The regions for SHEs in question are dominated by α decay. And α decay will be modified by only a factor of up to approximately 100, if the double shell closure will not be located at $Z = 114$ and $N = 184$.

The line of reasoning is, however, different concerning the production cross-section. The survival probability of the compound nucleus (CN) is determined among other factors significantly by the fission-barrier. Therefore all present calculations of cross-sections suffer from the uncertainty related with the location and strength of closed shells. However, it may also turn out that shell effects in the region of SHEs are distributed across a number of subshell closures. In that case a wider region of less deep shell-correction energy would exist with corresponding modification of stability and production yield of SHEs.

4. Nuclear reactions

4.1. Projectile-target combinations

Compound nuclei that could be produced concerning the availability of beams and targets are plotted in Fig. 4. The graphs also demonstrate the extension in the region of SHEs which will become possible with radioactive beams. The nuclei presently known or under investigation are marked by squares.

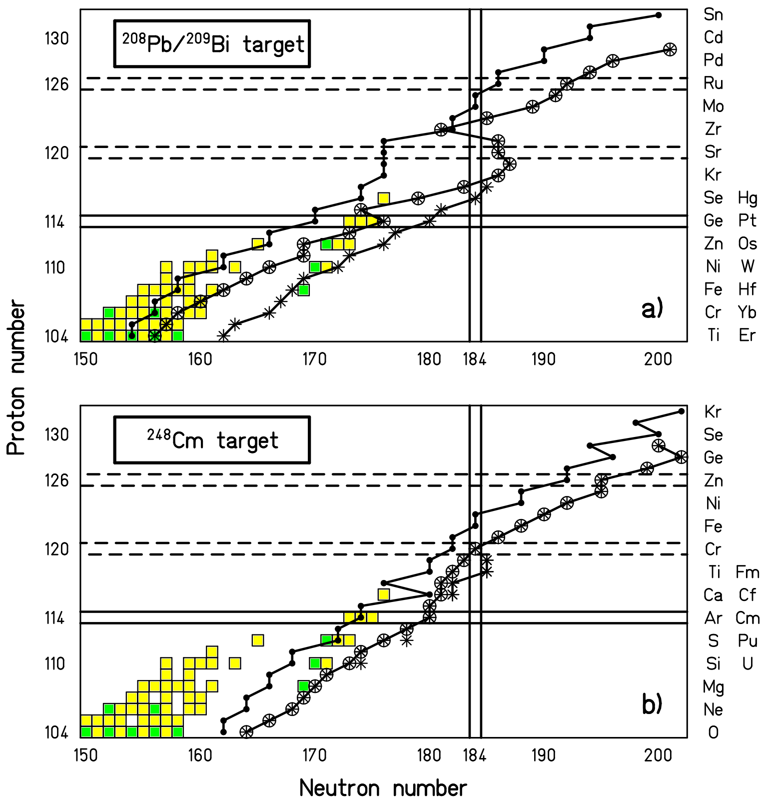

Fig. 4. Most neutron rich compound nuclei produced in reactions using stable and radioactive beams and targets (see text for an explanation of the symbols).

In Fig. 4(a) the curve marked with dots (•) shows the most neutron rich CN that can be produced with ^{208}Pb or ^{209}Bi targets and beams of the most neutron rich stable isotopes of the elements from Ti to Sn, given in the first column at the right ordinate. The double magic SHEs could be reached only if located at $Z = 126$ and $N = 184$.

On the average the accessible region is extended by 4 to 5 neutrons to the right using radioactive isotopes of the elements from Ti to Sn (symbol

$\otimes$ in Fig. 4(a)). As possible most neutron rich radioactive projectiles those isotopes were taken into account that could be produced with intensities of at least 10^9 /s according to the data presented in the RIA proposal [49].

Striking is the wide extension of possible CN to the neutron rich side at $Z = 120$ using beams of Kr, Rb and Sr. The reason is that these nuclei are available as fission fragments and can be accelerated with high yield, too. SHEs both at $Z = 120$ and 126 are well covered using reactions with Pb and Bi targets and radioactive beams.

More neutron rich nuclei of elements below $Z = 118$ can be produced using the radioactive beams of ^{96}Kr or ^{98}Rb and targets of stable neutron rich isotopes of elements below Pb from Hg down to Er (second column on the right ordinate, curve marked with symbol $*$). In these reactions evaporation residues could be produced in a region, where the new chains from element 114 and 116 are ending in the unknown. In this region α decay and spontaneous fission is expected with half-lives from seconds to hours (see Fig. 3).

In the lower plot, Fig. 4(b), the equivalent combinations are given for reactions using a ^{248}Cm target and stable and radioactive beams. Concerning the location of CN, no significant extension into the direction of neutron rich SHEs results from using radioactive beams compared with the reactions given in Fig. 4a. Apparent from the graph (Fig. 4(b)) is the extraordinary use of ^{48}Ca for the synthesis of neutron rich SHEs. The surplus of neutrons beyond ^{48}Ca can be only slightly increased using radioactive beams.

Radioactive beams of ^{47}K and ^{46}Ar are likely produced with high yield. Using these beams and in principle feasible actinide targets from U to Fm (the elements are given in the second column at the right ordinate) the surplus of neutrons can be further increased (CN marked by symbol $*$). However, selecting a reaction using actinide targets, one has to consider the availability of the material and the tremendous increase of safety problems in the handling of targets from U to Cf, Es or Fm.

Finally, we have to notice that SHEs at $Z = 114$ and $N = 184$ can be reached also not in reactions with radioactive actinide targets and radioactive beams. Concerning the CN on the right from $N = 184$ one has to keep in mind that the fission barrier vanishes rapidly with neutron number, and therefore these nuclei cannot be synthesized.

4.2. Cross-sections, fusion valleys, and excitation energy

The main features which determine the fusion process of heavy ions are (1) the fusion barrier and related beam energy and excitation energy, (2) the ratio of surface tension *versus* Coulomb repulsion which determines the fusion probability and which strongly depends from the degree of asymmetry of the reaction partners (the product Z_1Z_2 at fixed $Z_1 + Z_2$), (3) the impact parameter and related angular momentum, and (4) the ratio of neutron evaporation *versus* fission probability of the CN. In fusion of SHEs the product $Z_1 Z_2$ reaches extremely large and the fission barrier extremely small values. In addition, the fission barrier is fragile at increasing excitation energy and angular momentum, because it is solely built up from shell effects. For these reasons the fusion of SHEs is hampered, whereas the fusion of lighter elements is advanced through the contracting effect of surface tension.

The effect of Coulomb repulsion on the cross-section starts to act severely for fusion of elements beyond Fm. From there on a continuous decrease of cross-section was measured from microbarns for the synthesis of nobelium down to picobarns for the synthesis of element 112. The data obtained in reactions with ^{208}Pb and ^{209}Bi for the 1n evaporation channel at low excitation energies of about 10–15 MeV (therefore named *cold fusion*) and in reactions with actinide targets for the 4n channel at excitation energies of 35–45 MeV (*hot fusion*) are plotted in Fig. 5. Interesting for further investigation of SHEs are the relatively high cross-sections measured for the synthesis of elements 114 and 116 (4n channel) [46–48]. In both cases the obtained values of about 0.5 pb deviate considerably from the trend set by fusion of the lighter elements. An explanation could be a relatively high and wide fission barrier of the CN which is created by strong shell effects in the region of spherical SHEs. Note in this context that the experimental sensitivity increased by three orders of magnitude since the 1982–83 search experiments for element 116 using a hot fusion reaction [50].

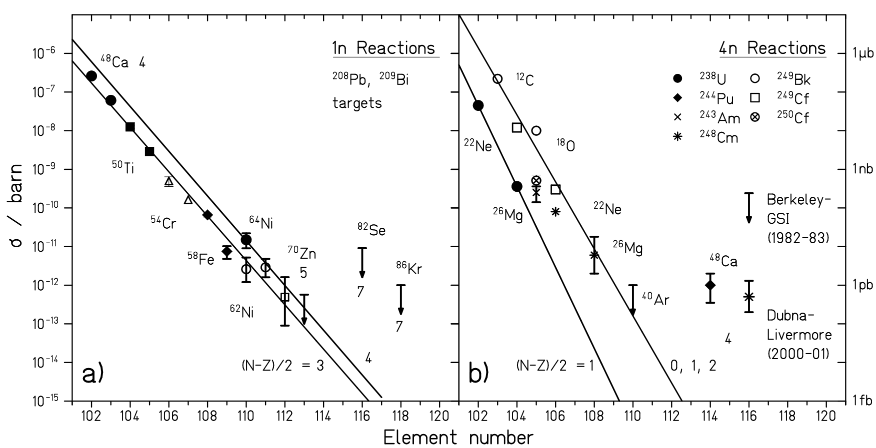

Fig. 5. Measured cross-sections and cross-section limits for reactions using ^{208}Pb and ^{209}Bi targets and one neutron evaporation (a) and for reactions using actinide targets and four neutron evaporation (b).

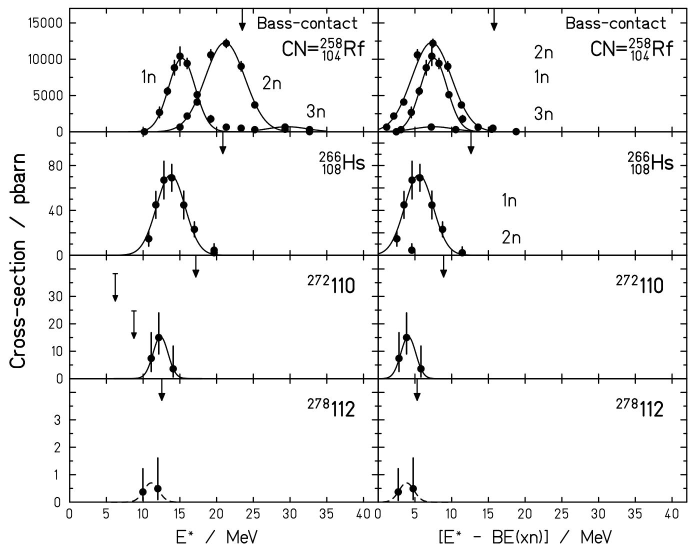

Fig. 6. Measured even element excitation functions.

A number of excitation functions was measured for the synthesis of elements from rutherfordium to 110 using Pb and Bi targets [32]. For the even elements these data are shown in Fig. 6. The maximum evaporation residue cross-section ($1n$ channel) was measured at beam energies well below a fusion barrier calculated in one dimension [16]. At the optimum beam energy projectile and target are just reaching the contact configuration in a central collision. The relatively simple fusion barrier based on the Bass model [16] is too high and a tunnelling process through this barrier cannot explain for the measured cross-section.

Various processes are possible and are discussed in the literature which result in a lowering of the fusion barrier. Among these transfer of nucleons and excitation of vibrational degrees of freedom are the most important [19–27,51]. The theoretical studies are also aimed at reproducing the known cross-section data and further extrapolating the calculations into the region of spherical superheavy nuclei. The measured cross-sections for the formation of ^{257}Rf up to ^{277}112 are reproduced almost within about a factor of 2 by the various models. However, there are significant differences in the cross-section values for the synthesis of spherical SHEs beyond $Z = 114$.

In the case of actinide targets, the target nucleus is strongly deformed and the height of the Coulomb barrier is a function of the orientation of the deformation axes. The reaction ^{48}Ca + ^{248}Cm was studied in Dubna [46,47], and evidence for the 4n channel was obtained at a beam energy resulting in an excitation energy of 30.4–35.8 MeV. Excitation functions were not yet measured.

It was pointed out in the literature [17] that closed shell nuclei as projectile and target are favorable for fusion of SHEs. The reason is not only a low reaction Q value and thus low excitation energy, but also that fusion of such systems is connected with a minimum of energy dissipation. The fusion path is along cold fusion valleys on the potential energy surface, where the reaction partners keep kinetic energy up to the closest possible distance. In this view the difference between *'cold'* and *'hot'* fusion is not only a result from different values of the excitation energy, but there exists also a qualitative difference, which is on the one side based on a well ordered fusion process along paths of minimum dissipation of energy (cold fusion), and on the other side on a process governed by the formation of a more or less energy equilibrated CN (hot fusion). This qualitative explanation is well in agreement with the results from experimental studies of quasi-fission and compound-nucleus fission [52].

Two features follow from the above concerning radioactive beams which probably modify the reaction cross-section in different ways. (1) Neutron rich projectiles result in CN with higher and wider fission barrier and thus result in an increase of the cross-section. (2) The desired transfer for initializing fusion is a transfer of protons from the projectile to the target. However, in neutron rich projectiles the protons are strongly bound and transfer of protons is more likely from the target to the projectile which will increase the Coulomb repulsion. This effect will increase the cross-section for quasi-elastic and deep-inelastic processes at the expense of fusion.

5. Summary and outlook

Experimental work of the last two decades has shown that the cross-sections for the synthesis of the heaviest elements decrease almost continuously. However, the recent data on the synthesis of element 114 and 116 in Dubna using hot fusion seem to break this trend when the region of spherical superheavy elements is reached.

The progress towards the exploration of the island of spherical SHEs is difficult to predict. However, one can hope that, during the coming years, more data will be measured in order to promote a better understanding of the stability of the heaviest elements and the processes that lead to fusion. The microscopic description of the fusion process will be needed for an effective explanation of the measured phenomena in the case of low dissipative energies. Then, the relationships between fusion probability and stability of the fusion products may also become apparent.

An opportunity for the continuation of experiments in the region of SHEs at decreasing cross-sections will be afforded by further accelerator developments. High current beams and radioactive beams are the options for the future. At increased beam currents, values of tens of particle μA's may become possible, the cross-section level for the performance of experiments can be shifted down into the region of tens of femtobarns, and excitation functions can be measured on the level of tenths of picobarns. The high currents, in turn, require the development of a new target and improvement of the separator. The radioactive beams, not as intense as the stable beams, will allow for approaching the closed neutron shell $N = 184$ already at lighter elements. Interesting will be the study of the fusion process using unstable neutron rich beams.

The half-lives of SHEs are expected to be relatively long. Based on nuclear models, which are effective predictors of half-lives in the region of the heaviest elements, values from microseconds to years have been calculated for various isotopes. This wide range of half-lives encourages the application of a wide variety of experimental methods in the investigation of SHEs, from the safe identification of short lived isotopes by recoil-separation techniques to exact mass measurements and atomic physics experiments on trapped ions, and to the investigation of chemical properties of SHEs using long-lived isotopes.

The recent experiments at SHIP were performed in collaboration with D. Ackermann, F.P. Heßberger, B. Kindler, J. Kojouharova, B. Lommel, R. Mann, G. Münzenberg, S. Reshitko, H.J. Schött (GSI Darmstadt); A. Popeko, A. Yeremin (JINR Dubna); S. Antalic, P. Cagarda, S. Saro (University Bratislava); M. Leino, J. Uusitalo (University Jyväskylä). During the years spent in preparing, performing, and analyzing experiments on the synthesis of heavy elements, we all benefitted substantially from discussions with Adam Sobiczewski to whom this paper is dedicated. We are particularly grateful for his advice in all questions related with the understanding of nuclear properties. We wish Adam all the best for his future.

REFERENCES

[1] A. Sobiczewski *et al.*, *Phys. Lett.* **22,** 500 (1966).

[2] S.G. Nilsson *et al.*, *Nucl. Phys.* **A115,** 545 (1968).

[3] A. Sobiczewski, *Physica Scripta* **10A**, 47 (1974).

[4] A. Sobiczewski *et al.*, *Phys. Lett.* **B224,** 1 (1989).

[5] A. Sobiczewski, *Phys. Part. Nucl.* **25**, 295 (1994).

[6] A. Sobiczewski *et al.*, *J. Alloys Comp.* **213/214**, 38 (1994).

[7] R. Smolanczuk *et al.*, *Phys. Rev.* **C52,** 1871 (1995).

[8] P. Möller and J.R. Nix, *Atomic Data and Nucl. Data Tables* **26,** 165 (1981).
[9] P. Möller *et al.*, *Atomic Data and Nucl. Data Tables* **59,** 185 (1995).
[10] P. Möller *et al.*, *Atomic Data and Nucl. Data Tables* **66,** 131 (1997).
[11] I. Muntian *et al.*, *Phys. Lett.* **B500,** 241 (2001).
[12] S. Cwiok *et al.*, *Nucl. Phys.* **A611,** 211 (1996).
[13] G.A. Lalazissis *et al.*, *Nucl. Phys.* **A608,** 202 (1996).
[14] K. Rutz *et al.*, *Phys. Rev.* **C56,** 238 (1997).
[15] A.T. Kruppa *et al.*, *Phys. Rev.* **C61,** 034313 (2000).
[16] R. Bass, *Nucl. Phys.* **A231,** 45 (1974).
[17] R.K. Gupta *et al.*, *Z. Phys.* **A283,** 217 (1977).
[18] von Oertzen, W.: *Z. Phys.* **A342,** 177 (1992).
[19] Y. Aritomo *et al.*, *Phys. Rev.* **C59,** 796 (1999).
[20] E.A. Cherepanov, *Pramana J. Phys.* **53,** 619 (1999).
[21] R. Smolanczuk, *Phys. Rev.* **C59,** 2634 (1999).
[22] R. Smolanczuk, *Phys. Rev. Lett.* **83,** 4705 (1999).
[23] G. Giardina *et al.*, *Eur. Phys. J.* **A8,** 205 (2000).
[24] V.Yu. Denisov and S. Hofmann, *Phys. Rev.* **C61,** 034606 (2000).
[25] G.G. Adamian *et al.*, *Nucl. Phys.* **A678,** 24 (2000).
[26] G.G. Adamian *et al.*, *Phys. Rev.* **C62,** 064303 (2000).
[27] R. Smolanczuk, *Phys. Rev.* **C63,** 044607 (2001).
[28] V.I. Zagrebaev, *Phys. Rev.* **C64,** 034606 (2001).
[29] V.Yu. Denisov and W. Nörenberg, *Eur. Phys. J.* A, submitted (2002).
[30] G. Münzenberg *et al.*, *Nucl. Instr. Meth.* **161,** 65 (1979).
[31] S. Hofmann, *Z. Phys.* **A291,** 53 (1979).
[32] S. Hofmann and G. Münzenberg, *Rev. Mod. Phys.* **72,** 733 (2000).
[33] G. Münzenberg, *Rep. Prog. Phys.* **A51,** 57 (1988).
[34] S. Hofmann, *Rep. Prog. Phys.* **A61,** 639 (1998).
[35] S. Hofmann *et al.*, *Z. Phys.* **A350,** 277 (1995).
[36] S. Hofmann *et al.*, *Eur. Phys. J.* **A10,** 5 (2001).
[37] S. Cwiok *et al.*, *Phys. Rev. Lett.* **83,** 1108 (1999) and private communication.
[38] S. Hofmann *et al.*, *Z. Phys.* **A350,** 281 (1995).
[39] S. Hofmann *et al.*, *Eur. Phys. J.* **A14,** 147 (2002).
[40] S. Hofmann *et al.*, *Z. Phys.* **A354,** 229 (1996).
[41] A. Türler *et al.*, *Eur. Phys. J.* , submitted (2002).
[42] Ch.E. Düllmann *et al.*, *Nature* **418,** 859 (2002).
[43] V. Ninov *et al.*, *Phys. Rev. Lett.* **83,** 1104 (1999).
[44] V. Ninov *et al.*, *Phys. Rev. Lett.* **89,** 039901 (2002).

[45] R. Smolanczuk and A. Sobiczewski, Proc. XV. Nucl. Phys. Divisional Conf. on *Low Energy Nuclear Dynamics*, St.Petersburg, Russia, April, 1995, (World Scientific, Singapore, 1995) p. 313.

[46] Yu.Ts. Oganessian *et al.*, *Phys. Rev.* **C63,** 011301 (2000).

[47] Yu.Ts. Oganessian *et al.*, *Phys. Atomic Nuclei* **64**, 1349 (2001).

[48] Yu.Ts. Oganessian *et al.*, *Nature* **400,** 242 (1999).

[49] RIA, *The Rare Isotope Accelerator Project,* www.phy.anl.gov/ria (2000).

[50] P. Armbruster *et al.*, *Phys. Rev. Lett.* **54,** 406 (1985).

[51] V.I. Zagrebaev, in *Proc. Int. Workshop on Fusion Dynamics at the Extremes*, Dubna, Russia, May, 2000, (World Scientific, 2001) p. 215.

[52] M.G. Itkis *et al.*, in *Proc. Int. Workshop on Fusion Dynamics at the Extremes*, Dubna, Russia, May, 2000, (World Scientific, 2001) p. 93.